EFDA-JET-CP(07)01-12

M. Laxåback and JET EFDA Contributors

Predictive Analysis of High Power ICRF Heating in JET

Predictive Analysis of High Power ICRF Heating in JET

M. Laxåback[1] and JET EFDA Contributors*

[1]*EFDA-CSU, Culham Science Centre, Abingdon UK;*
also Association EURATOM-VR, EES, KTH, Stockholm Sweden
** See annex of M. Watkins et al, "Overview of JET Results ",*
(Proc. 21st IAEA Fusion Energy Conference, Chengdu, China (2006).

Preprint of Paper to be submitted for publication in Proceedings of the
17th Topical Conference on Radio Frequency Power in Plasmas,
(Clearwater, Florida, USA, 7-9th May 2007)

ABSTRACT

One aim of the 2007 JET shutdown is to increase the ICRF power by installing a new, internally matched, two-strap antenna and by adding external conjugate-T matching to two of the four A2 antennas for improved ELM-resilience. The new so-called ITER-like antenna is designed to deliver 7.2MW to the plasma which, together with the A2 antenna improvements, effectively doubles the power available for ICRF heating. At the resulting power densities the resonant ion power partition, the collisional bulk plasma ion and electron heating fractions and profiles are all affected.With the increased power more resonant ions are accelerated to higher energies, leading to an increased electron heating fraction and, due to the wider ion orbits, broader heating profiles. The heating asymmetries with directed antenna spectra are enhanced, partly due to the higher power and thereby larger toroidal momentum transfer between wave and ions, and partly due to the reduced pitch-angle scattering of the higher-energy ions. Here, coupled wave field and resonant ion distribution function calculations are presented for JET Advanced Tokamak scenarios, where the low central current densities and associated broad fast ion orbits increase the impact of the power density, and analysed to determine to what extent the increased power density will affect the heating.

INTRODUCTION

The JET programme is focused on evaluating ITER technologies and on the preparation of ITER plasma operating scenarios. The installation of a new ICRF antenna in 2007 is expected to progress both these topics; by providing experience in operating an antenna of a design similar to that foreseen for ITER on a plasma that is as close as possible to that expected in ITER and by allowing the JET plasma to approach the foreseen ITER plasma in dimensionless parameters through the increase in electron heating in the otherwise predominantly Neutral Beam heated JET plasmas. This study focuses on the latter topic, analysing the effects of the increased power density on the plasma heating, the non-thermal neutron yield and on the power lost to the wall for a selection of common heating scenarios. Possible wall losses at the higher power densities are of particular concern due to the pending installation of an all-metal wall in JET. Previously, the impact of the increased ICRF power on future DT experiments has been analysed using the same numerical tools that are used for routine ICRF analysis at JET [1]. These do not take into account the toroidal momentum exchange between the wave field and the ions, nor complete orbit effects, and a further aim of the present study is therefor to assess whether the inclusion of these effects will be necessary for routine analysis of future high power JET discharges.

THE SELFO CODE

SELFO [2, 3] models ICRH by self-consistently coupling the FIDO Monte-Carlo code [4] to the LION global wave code [5, 6]. FIDO calculates the resonant ion distribution functions, including broad ion drift orbits and the exchange of toroidal momentum with the wave, for a given wave field spectrum and computes their dielectric tensor susceptibility contributions assuming a quasi-

homogeneous plasma with $k_{\|}$ approximated $n\phi/R$ and $k_{\perp}$ taken from the fast wave dispersion relation. Wave fields and power partition on resonant species are iteratively updated by LION using the computed dielectric tensor.

INCREASED ICRF POWER IN AT SCENARIOS

JET Advanced Tokamak scenario development aims at achieving ITER-relevant steadystate plasmas, i.e. $q_{95} \approx 5$, optimised or weakly reversed shear, $T_e \approx T_i$ and relatively high densities as well as ELM control for metal wall compatibility [7]. The basis for this study, pulse #67863, was a typical example. At t = 46.7 s the main plasma parameters were: B_0 = 3T, I_p = 2MA, T_i = 7.7keV, T_e = 7.5keV, n_e = 4.4×10^{19}m^{-3} and P_{NBI} = 19MW. The ICRH scenario was H minority in D and Ne puffing was used for Type-III ELMs. Z_{eff} = 3 and n_H/n_D =5% has been assumed unless otherwise noted.

Dependence on phasing at 3 T / 2MA, 46MHz, central resonance

Interactions with toroidally directed waves change the toroidal canonical momentum, $P\phi = mRv\phi - ZeΨ$, of resonant ions [8, 9], notably driving turning points of trapped ions inwards (outwards) with co- (counter) current propagating waves. Table 1 compares key results from simulations with dipole, +90° (co-current) and –90° (counter-current) phasings for the current and future RF powers, 7MW/ 14MW, as well as a NBI-only reference; fast energy content, power partition on H minority and D beam and bulk ions, DD neutron rate, bulk electron heating, radius inside which half the collisional electron heating is deposited and the wall power load from orbit losses. At the higher power

TABLE 1. Dependence on antenna phasing at 7MW/14MW ICRF power

	W_{fast} (MJ)	P_H (%)	P_D (%)	R_N (e16)	P_e (MW)	$\frac{r}{a}$ ($\frac{1}{2}$ P_e)	P_{wall} (MW)
Dipole	1.9 / 2.7	74 / 75	19 / 19	1.8 / 2.1	12.0 / 17.8	0.49 / 0.49	0.57 / 0.65
+90°	2.1 / 3.1	69 / 64	26 / 32	2.0 / 2.7	12.1 / 17.9	0.47 / 0.46	0.60 / 0.63
–90°	1.9 / 2.6	77 / 74	19 / 22	1.8 / 2.2	12.0 / 17.5	0.51 / 0.51	0.63 / 0.91
NBI	1.1	–	–	1.4	7.3	0.59	0.59

the differences between the phasings are amplified, with a higher relative fast energy content and neutron yield with +90° and higher wall loading with –90°. Notably, the bulk electron heating profiles are only weakly affected by the increased power. This can be attributed to the gradient in the static temperature profiles and the progressively increased drag experienced by broad orbits extending outside the mid radius.

Dependence on resonance position at 3 T / 2MA, dipole phasing

Off-axis ICRH is frequently used to achieve broader electron heating, e.g. to control the current diffusion rate and the *q*-profile, or to avoid triggering Alfvén eigenmodes. Table 2 compares the heating with the resonance in the centre to that with it 30% off-axis.

TABLE 2. Dependence on resonance position at 7MW/14MW ICRF power

	W_{fast} (MJ)	P_H (%)	P_D (%)	R_N (e16)	P_e (MW)	$\frac{r}{a}$ ($\frac{1}{2} P_e$)	P_{wall} (MW)
HFS	*1.9 / 2.8*	*66 / 68*	*20 / 19*	*1.9 / 2.2*	*12.2 / 18.2*	*0.49 / 0.46*	*0.59 / 0.66*
Centre	*1.9 / 2.7*	*74 / 75*	*19 / 19*	*1.8 / 2.1*	*12.0 / 17.8*	*0.49 / 0.49*	*0.57 / 0.65*
LFS	*1.8 / 2.5*	*55 / 47*	*41 / 50*	*2.1 / 2.9*	*11.5 / 16.7*	*0.52 / 0.53*	*0.64 / 1.14*

High field side and central heating are here very similar. With the resonance on the low field side however, at a lower magnetic field and subsequently with larger Larmor radii, the higher power leads to increased second harmonic D damping, higher neutron yield and increased wall losses, predominantly in the form of RF accelerated beam ions.

Dependence on plasma current, central resonance, dipole phasing

The effect of different plasma currents are illustrated in table 3, where the magnetic field has been scaled to keep the *q*-profile constant. Lower plasma currents imply broader

TABLE 3. Dependence on plasma current at 7MW/14MW ICRF power

	W_{fast} (MJ)	P_H (%)	P_D (%)	R_N (e16)	P_e (MW)	$\frac{r}{a}$ ($\frac{1}{2} P_e$)	P_{wall} (MW)
1.6MA	*1.8 / 2.4*	*59 / 62*	*28 / 27*	*1.9 / 2.2*	*11.6 / 17.2*	*0.51 / 0.52*	*0.80 / 1.03*
2.0MA	*1.9 / 2.7*	*74 / 75*	*19 / 19*	*1.8 / 2.1*	*12.0 / 17.8*	*0.49 / 0.49*	*0.57 / 0.65*
2.3MA	*2.0 / 2.8*	*80 / 80*	*14 / 16*	*2.1 / 2.9*	*12.5 / 18.0*	*0.48 / 0.47*	*0.41 / 0.41*

orbits and higher losses. This is confirmed by the simulations, where the heating profiles are broader and the fast ion losses are 2.5 times higher at 1.6MA than at 2.3MA. The lower magnetic fields at the lower currents also lead to increased RF acceleration of D beam ions. Again, these make up the bulk of the wall power load.

Notes on the minority concentration

Three scenarios above indicate a possible problem with the wall power load at high RF power; –90°

phasing, LFS resonance and low plasma current. Fortunately, as table 4 illustrates, these problems can be alleviated by increasing the minority concentration, as this reduces the power density on both resonant species and thereby the wall loading.

TABLE 4. Increased minority concentration, 5%/ 7.5% H, at 14MW ICRF power

	W_{fast} (MJ)	P_H (%)	P_D (%)	R_N (e16)	P_e (MW)	$\frac{r}{a}$ ($\frac{1}{2}$ P_e)	P_{wall} (MW)
–90°	*2.6 / 2.6*	*74 / 84*	*22 / 13*	*2.2 / 1.9*	*17.5 / 17.5*	*0.51 / 0.49*	*0.91 / 0.76*
LFS	*2.5 / 2.5*	*47 / 58*	*50 / 39*	*2.9 / 2.6*	*16.7 / 16.1*	*0.53 / 0.52*	*1.14 / 0.79*
1.6MA	*2.4 / 2.4*	*62 / 71*	*27 / 19*	*2.3 / 2.1*	*17.2 / 16.8*	*0.52 / 0.50*	*1.03 / 0.84*

Conversely, decreasing the minority concentration could be expected to significantly increase the wall loading. This is however not necessarily the case, as table 5 indicates. With good fast ion confinement the wall losses are dominated by D beam ions, c.f. table 1. Decreasing the minority concentration increases the power density on the D ions, but since the losses above the NBI-only losses are moderate to start with, this need not significantly change the total wall power loading.

TABLE 5. Decreased minority concentration, 5%/ 2.5% H, at 14MW ICRF power

	W_{fast} (MJ)	P_H (%)	P_D (%)	R_N (e16)	P_e (MW)	$\frac{r}{a}$ ($\frac{1}{2}$ P_e)	P_{wall} (MW)
Dipole	*2.7 / 2.7*	*75 / 50*	*19 / 41*	*2.1 / 3.0*	*17.8 / 17.0*	*0.49 / 0.50*	*0.65 / 0.76*
2.3MA	*2.8 / 2.9*	*80 / 54*	*16 / 40*	*2.0 / 3.0*	*18.0 / 17.5*	*0.47 / 0.49*	*0.41 / 0.54*

CONCLUSIONS

In general, the additional ICRF power should not significantly change the characteristics of the heating, indicating that the present analysis tools should be able to treat these scenarios adequately. The heating profiles are similar, given the same background plasma, and wall losses are moderately enhanced. Excessive wall losses in difficult scenarios can be avoided by increasing the minority concentration. In scenarios with good fast ion confinement the risk to the wall from fast ion losses should be manageable.

REFERENCES

[1]. M.J. Mantsinen et al., In Proc. of the 29th EPS Conf. on Plasma Physics and Controlled Fusion, Vol. 26 B, P–1.033,Montreux, (2002)

[2]. J. Hedin et al., In Theory of Fusion Plasmas, 467, Varenna, (1998)

[3]. M. Laxåback and T. Hellsten, Nuclear Fusion, **45** 1510 (2005)

[4]. J. Carlsson et al., In Theory of Fusion Plasmas, 351, Varenna, (1994)

[5]. L. Villard et al., Computer Physics Reports, **4** 95 (1986)

[6]. L. Villard et al., Nuclear Fusion, **35** 1173 (1995)

[7]. X. Litaudon et al., In Proc. of the 21st IAEA Fusion Energy Conf., EX/P1–12, Chengdu, (2006)

[8]. M. Mantsinen et al., Nuclear Fusion, **40** 1773 (2000)

[9]. T. Hellsten, et al., Nuclear Fusion, **44** 892 (2004)

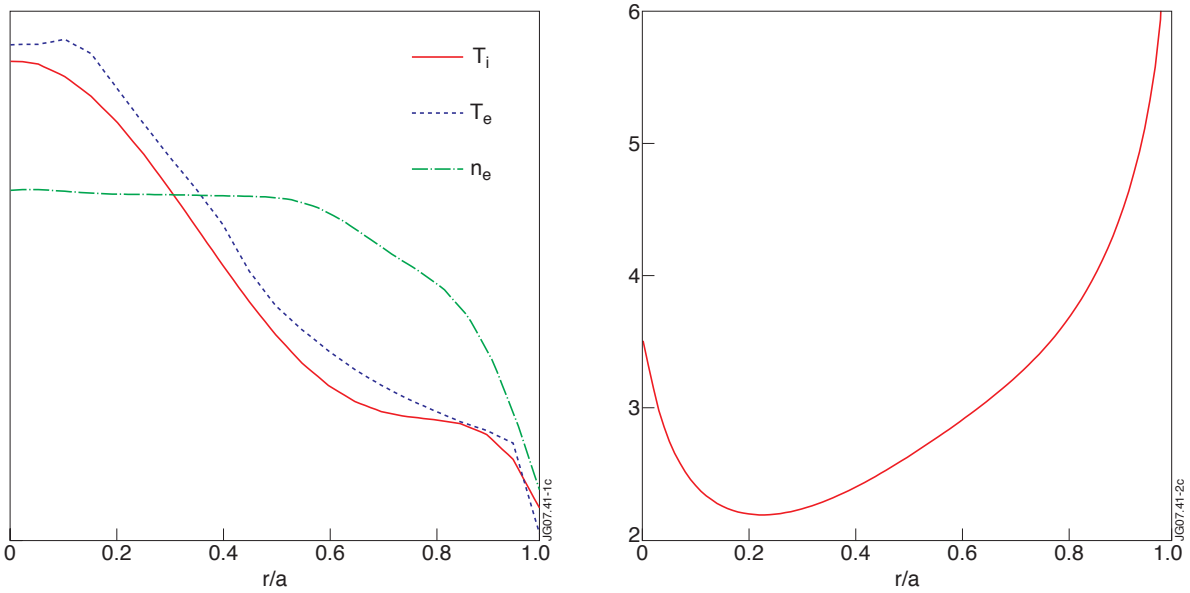

FIGURE 1. #67863 at t = 46.7 s. Left: Temperature and density profiles. Right: q profile.